EUS1- Joensuu, 19-23 August 2018

Fundamentals and applications of ion-molecule reactions

SAPIENZA
UNIVERSITÀ DI ROMA

EU FT-ICR MS

Maria Elisa Crestoni

Dipartimento di Chimica e Tecnologie del Farmaco, Università degli Studi di Roma "La Sapienza", P.le A. Moro 5, I-00185, Roma (Italy)

Ions are widely used in (in)organic reaction chemistry as:

- reactants
- intermediates
- catalysts

because they are highly reactive.

Solvation energies are very large (hundreds kcal/mol) and can mask differences in intrinsic reactivity between similar species.

By studying ionic reactions in the gas phase, without solvent and counterion, we can learn the intrinsic behavior in ionic reactions and expose the role of the environment.

ion-molecule reactions ⟺ mass spectrometry

mass spectrometry ⟷ solvent free environment

ion-molecule reactions → solvent free environment

IMPACT

fundamentals

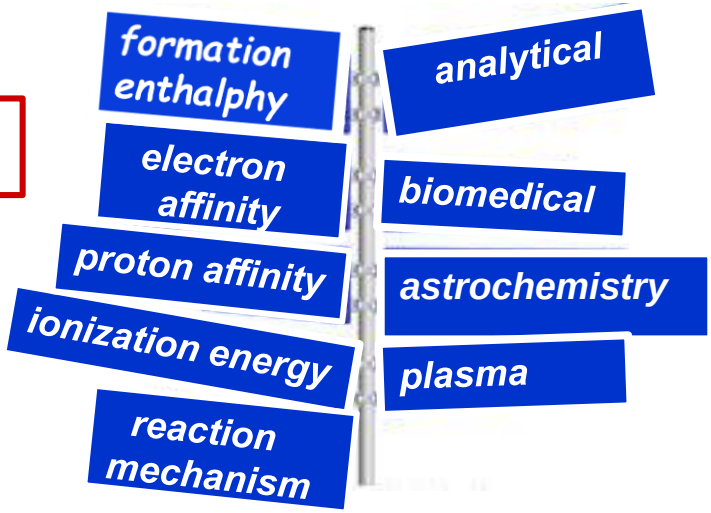

applied areas

J. S. Brodbelt, Mass Spectrom. Rev. 1997; S. Gronert, Chem. Rev. 2001; V. Ryzhov, Anal. Chem. 2013

IMR

Pros

- intrinsic properties
- sensitivity
- specificity
- speed
- efficiency
- infinite reaction-based strategies
- no extensive purification/sample preparation
- (indirect) structural information

Cons

- inferred information on neutral products
- volatile neutrals

Ion-trapping instruments (FT-ICR and ion-trap) are the most versatile for IMR studies:

- low pressure measurements (10^{-5}-10^{-8} torr)
- allow time and energy control of reactions
- mass selection of reactant and product ions
- structural characterization by CID
- multistep MS^n sequences
- in FT-ICR: high resolution, high mass accuracy mode of operation

Items

- Measure rate constants
- Determine the efficiency of the reaction
- Theory of ion-molecule capture/collision
- Slow/fast reactions: double minimum PES
- Types of IMR
- Applications of IMR

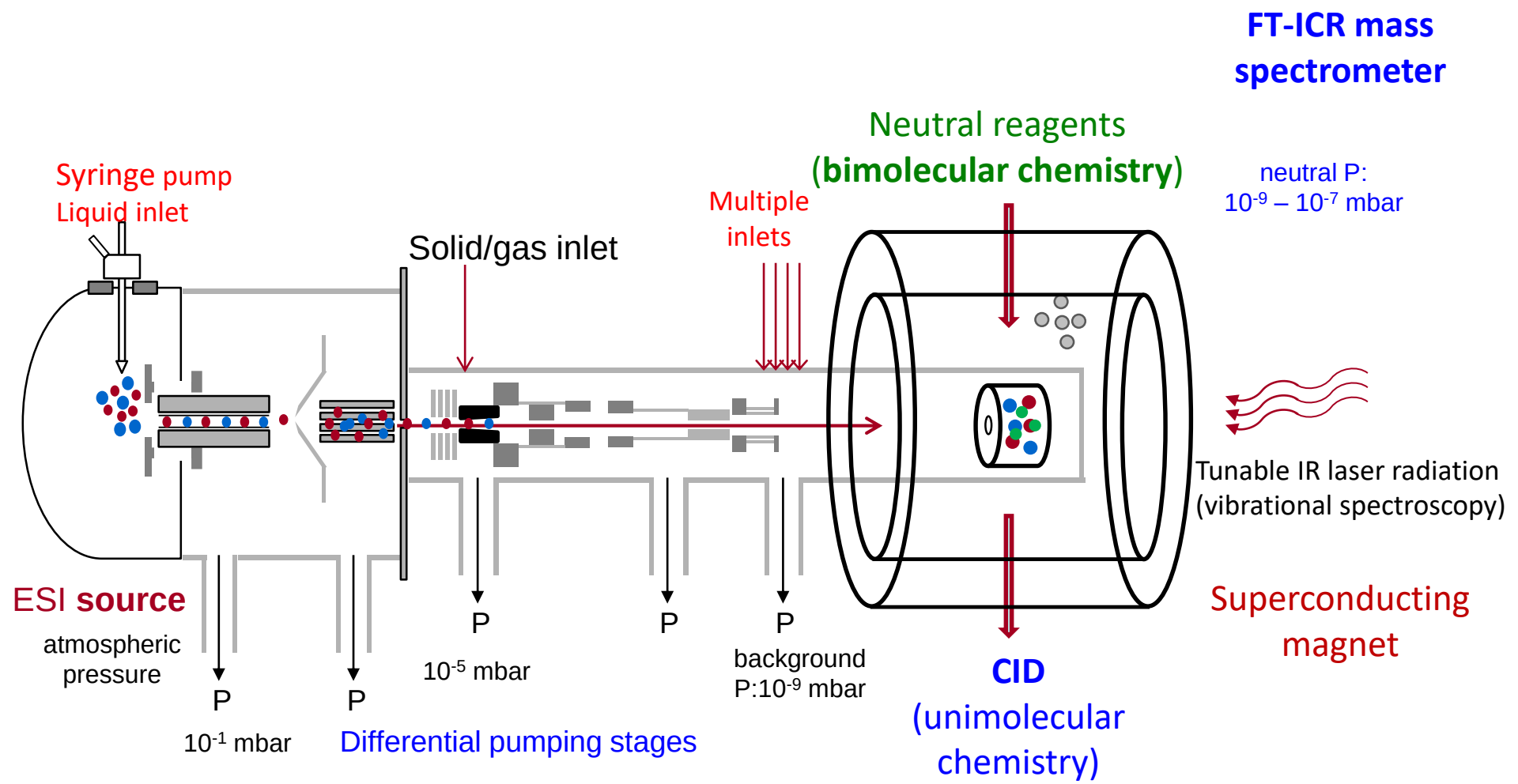
FT-ICR mass spectrometer
Neutral reagents
(bimolecular chemistry)
neutral P:
10-9 – 10-7 mbar
Syringe pump
Liquid inlet
Multiple inlets
Solid/gas inlet
Tunable IR laser radiation
(vibrational spectroscopy)
ESI source
atmospheric pressure
P
10-1 mbar
P
Differential pumping stages
P
10-5 mbar
P
P
background
P:10-9 mbar
CID
(unimolecular chemistry)
Superconducting magnet

Equipment for TNA in Roma

Reaction Rates

$R^+ + N \longrightarrow P^+ +$ neutral products

$$-\frac{dR(t)}{dt} = k\, n\, R(t)$$

the reaction is bimolecular

n = number density of neutral N

In a conventional bimolecular process the number density of neutral reactant would decrease with time. Here, it does not.

$$I_{(t)} = I_0\, e^{-nkt}$$

pseudo-first order reaction

$$\ln \frac{I_{(t)}}{I_0} = -\, n\, k\, t$$

$k = k_{exp}$

The total signal intensity is used to normalize the data and avoid errors from slight variations in the number of ions.

Monitoring the signal intensity of $I_{(t)}$ at a given time and following the progress of the reaction with the time, the rate constants for the disappearance of reactant ions and the appearance of product ions are obtained.

- The semilog plot of the decrease of the parent ion abundance with time is linearly interpolated and the **pseudo-first order rate constant** is obtained.
- The bimolecular rate constant (k_{exp}) at 300 K is gained from the ratio between the negative slope and ***n***, the number density of the neutral.
- ***n*** is calculated from the ideal gas equation and allows to convert the measured value of the neutral pressure (mbar) in molecule cm^{-3} at 300 K.

- $$k_{exp} = \frac{\text{- slope } (s^{-1})}{n \text{ (molecule cm}^{-3})} = \ldots. \text{ cm}^3 \text{ molecule}^{-1} \text{ s}^{-1}$$

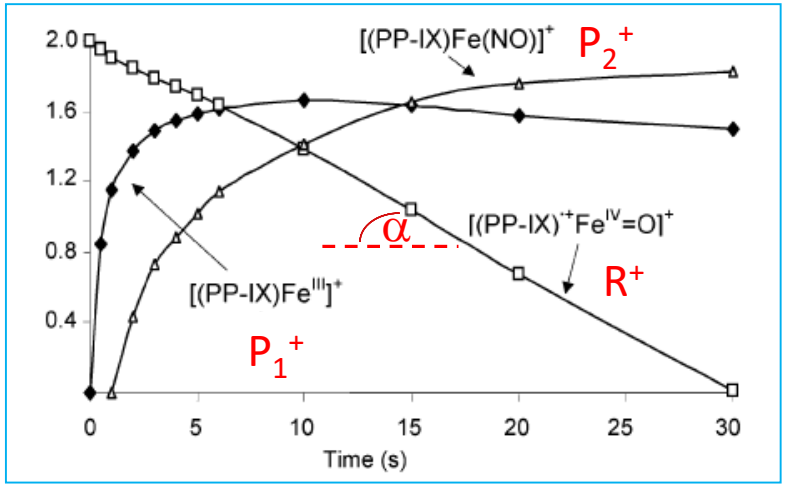

Figure 2. Plot of the logarithm of the relative ion abundances (%) versus time for the reaction of $(PP\text{-}IX)^{\bullet+}Fe^{IV}{=}O$ with NO at 3.0×10^{-8} mbar.

$$R^+ + NO \xrightarrow{OAT} P_1^+ + NO_2$$

$$P_1^+ + NO \xrightarrow{Add} P_2^+$$

Typically, the reproducibility of k_{exp} values is within 10%;

while the error in the absolute rate constants is estimated to be ± 30%.

It is mainly due to uncertainty in pressure measurements.

calibration of cold cathode gauge

$CH_4^{+\cdot} + CH_4 \longrightarrow CH_5^+ + CH_3$

$k_{CH4} = 1{,}1 \times 10^{-9}\ cm^3\ molecule\ s^{-1}$

time	I% m/z 16	I% m/z 17	ln 16
0	100.00	0.00	4.605
0.01	84.00	15.00	4.431
0.02	79.00	22.00	4.369
0.03	71.00	29.00	4.263
0.04	66.00	34.00	4.190
0.05	62.00	38.00	4.127
0.06	57.00	43.00	4.043
0.08	50.00	50.00	3.912
0.1	42.00	58.00	3.738
0.12	37.00	63.00	3.611
0.14	30.00	70.00	3.401
0.16	25.00	75.00	3.219
0.18	20.00	80.00	2.996
0.2	16.00	84.00	2.773
0.25	9.00	91.00	2.197
0.3	6.00	94.00	1.792
0.4	0.00	100.00	

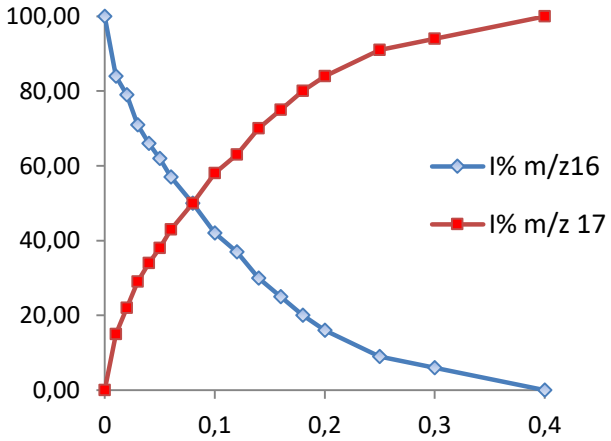

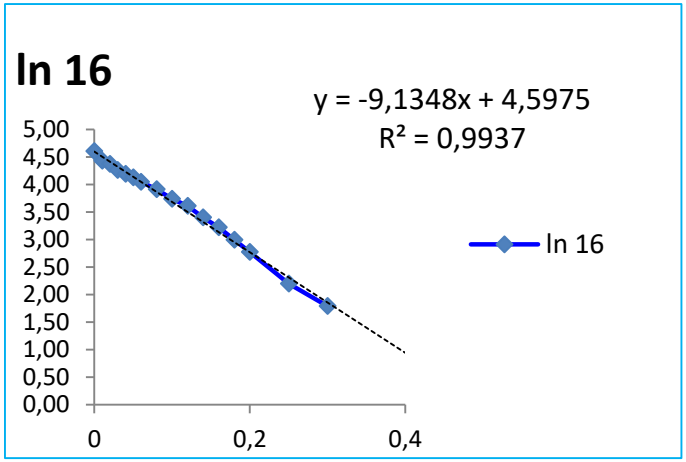

-slope

$$k_{exp} = \frac{9{,}13}{2{,}4 \times 10^{16} \times 1{,}1 \times 10^{-7}}\ cm^3\ molecule^{-1}\ s^{-1}$$

number density at 1.1×10^{-7} mbar

$K_{exp} / k_{CH4} = f$ (calibration factor)

The efficiency (Φ) of an ion molecule reaction can be determined by comparing the experimental rate constant (k_{exp}) with a theoretical estimate of the capture rate constant as percentages of the collision rate constant (k_{coll}).

$$\Phi = \frac{k_{exp}}{k_{coll}}$$

measure of reaction probability per collision
(number of events that bring to reaction)

Many exothermic reactions exhibit unit reaction probability at room T;

others proceed with reaction efficiency much less than unity.

Now we have to face two questions:

1) **how do we calculate k_{coll}**

2) **how do we explain the evidence that many exothermic reactions have unit efficiency whereas others present (very) low reaction efficiency**

Theoretical aspects of ion-molecule reactions

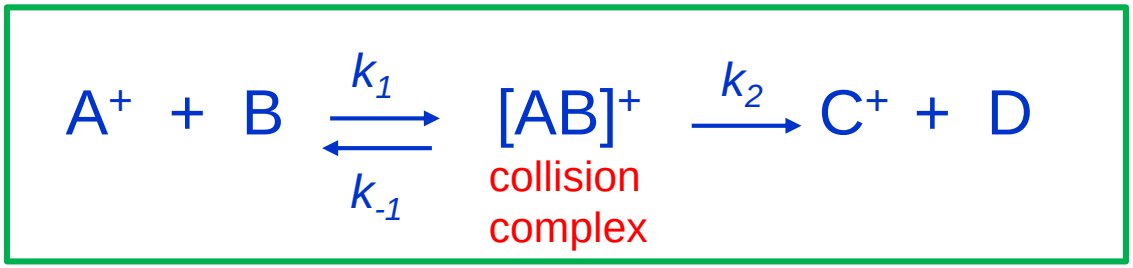

Capture/collision rate : k_{coll} ~ 1×10^{-9} cm^3 $molecule^{-1}$ s^{-1}

One or two order of magnitude larger than molecule-molecule reactions

Calculations of collision rate constant

- Ion/induced dipole potential: Langevin (and Gioumousis-Stevenson) theory
- Average dipole orientation (ADO) : Su & Bowers
- Angular momentum conserved ADO : Su & Chesnavich

Langevin Theory

$$V = \frac{-\alpha e^2}{2r^4}$$

potential energy of attraction

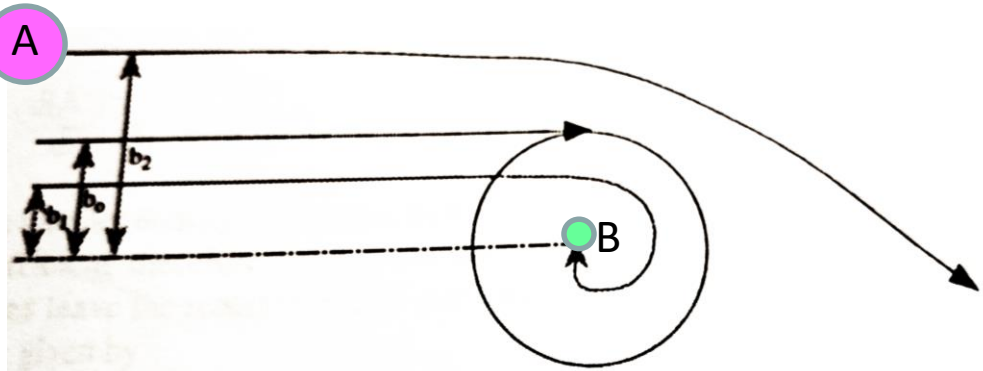

the two spheres will collide for $0 \le b \le b_C$

$$k_L = \int_0^\infty f(g)\,\sigma$$

σ = cross section = $\pi (r_A + r_B)^2 = \pi b_C^2$

area of the circle in the yz plane

f (g) = v_0 over a Maxwell distribution of velocities

b_C = critical value of impact parameter for collision

$b_C = (4e^2\alpha/\mu g^2)^{1/4}$

$b = b_C/\sqrt{2}$ (radius of the fixed orbit)

(μ= the reduced mass of the pair; g= relative velocity)

$$\sigma = \pi b_C^2 = (2\pi e/g)(\alpha/\mu)^{1/2}$$

collision cross section between a nonpolar molecule and an ion of charge e

for slow molecules, b_C and hence σ are greater

for IMR with no activation energy= reaction cross section (depends on α and g)

$$k_L = g\,\sigma = 2\pi e\left(\frac{\alpha}{\mu}\right)^{1/2}$$

capture rate coefficient

equation of Giomousis and Stevenson

The Langevin model does not deal with the case of molecules that have permanent dipole moments.

Locked dipole Theory

- it is assumed that the dipole is oriented toward the ion with a zero degree angle.
- maximization of dipole contribution: **excessively large calculated rate constants**
- Langevin treatment and “locked dipole” served to bracket capture limit rate constants of ion-polar molecule collisions

k_{ADO} Theory

ADO: averaged dipole orientation

- it is assumed that there is no net angular momentum transfer between the rotating molecule and the ion-molecule orbital motion
- statistical methods are used to calculate the average orientation of the polar molecule in the ion field
- predicts accurately absolute proton transfer rate constants

G. Giomousis, D. P. Stevenson, *J. Chem. Phys.* 1958

k_{ADO} Theory

ADO: averaged dipole orientation

$$V = \frac{-\alpha q^2}{2r^4} \quad \frac{-\mu_D q}{r^2} \cos\Theta$$

Θ is the instantaneous angle between the dipole and the line of interaction with the ion (in the locked dipole approximation $\cos\Theta = 1$). It varies with r.

the first term is the Langevin or induced dipole contribution

the second term reduces the dipolar contribution to V (average dipole energy)

$$k_{ADO} = \frac{2\pi q}{\sqrt{\mu}} \left\{ \sqrt{\alpha} + C\mu_D \left(\frac{2}{\pi k_B T} \right)^{1/2} \right\}$$

μ is the reduced mass; μ_D is the permanent dipole;
C is a correction factor that is function of $\mu_D / \alpha^{1/2}$;
k_B is Boltzmann's constant

T. Su, . T. Bowers, *J. Chem. Phys.* 1973; *Int. J. Mass Spectrom. Ion Phys.* 1973

k_{AADO} Theory

AADO: angular momentum conserved ADO

- there is a net angular momentum transfer between the rotating molecule and the ion-molecule orbital motion.
- the AADO theory yields capture rate constants larger than ADO theory
- the AADO equation represents the best means to obtain an estimated capture rate for comparison with experimental reaction rate constants (± 10%) .

$$k_{AADO} = k_L\, G(x)$$

$$G(x) = \frac{(x+0.509)^2}{10.526} + 0.9754 \qquad x < 2$$

$$G(x) = (x+0.509)^2 + 0.9754 \qquad x \geq 2$$

empirical parametrization

$$x = \frac{\mu_D}{(8\pi\varepsilon_0\alpha k_B T)^{1/2}}$$

T. Su, . W. J. Chesnavich, *J. Chem. Phys.* 1982

The double-well model for IMRs

Many exothermic ion-molecule reactions proceed at collision rates :

- ion-dipole and ion-induced dipole attraction at long range;
- large interaction energy at short range

Though, many counter-examples (slow rates) are known.

slow means that most of the collisions simply return back to reactants

$$X^- + CH_3Y \underset{k_{-1}}{\overset{k_1}{\rightleftharpoons}} X^- \bullet CH_3Y \underset{k_{-2}}{\overset{k_2}{\rightleftharpoons}} CH_3 X^\bullet Y^- \xrightarrow{k_3} CH_3X + Y^-$$

nucleophilic displacement (SN2)

Capture is a necessary but not sufficient condition for reaction…

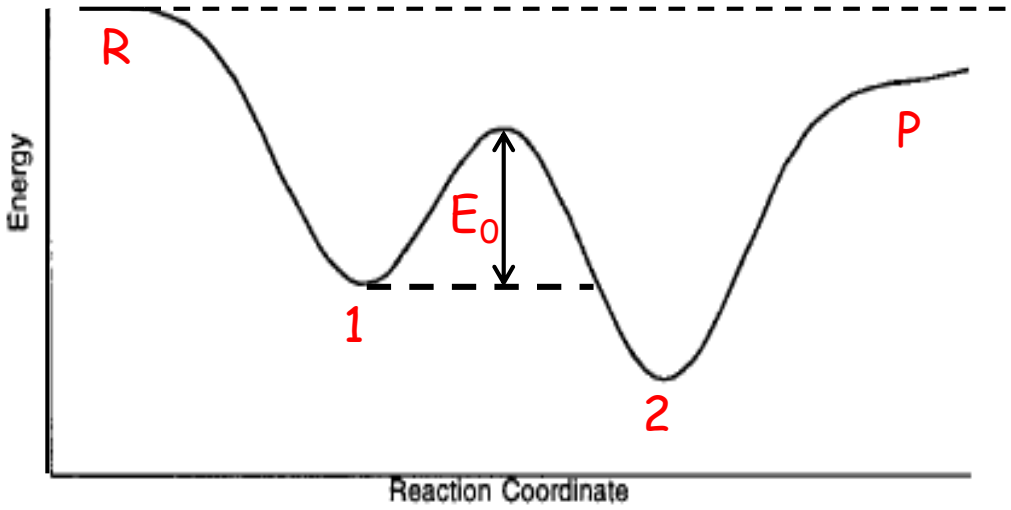

Gas-phase double-well potential energy surface.

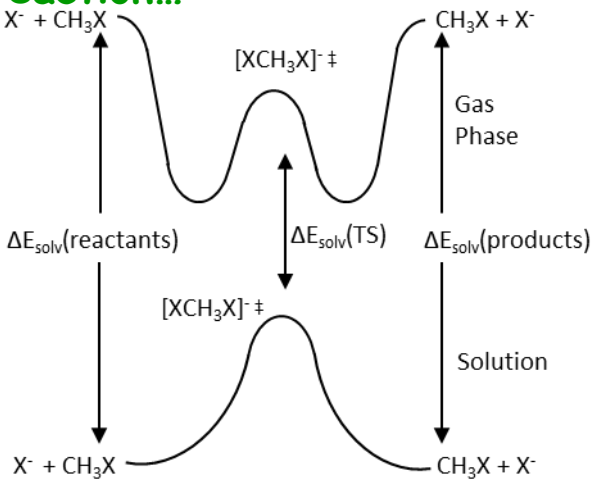

Gas-phase and solution PES for the SN2 reaction.

W. N. Olmstead, J. I. Brauman, *J. Am. Chem. Soc.* 1977

Overall the efficiency depends on the height of the central barrier and the entropic constraints at the transition state.

$$X^- + CH_3Y \underset{k_{-1}}{\overset{k_1}{\rightleftharpoons}} X^- \bullet CH_3Y \underset{k_{-2}}{\overset{k_2}{\rightleftharpoons}} CH_3X \bullet Y^- \xrightarrow{k_3} CH_3X + Y^-$$

R 1 2 P

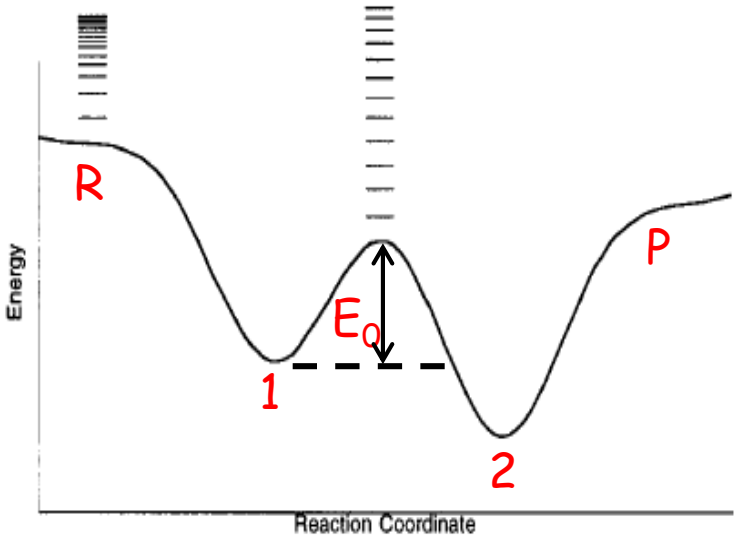

under the collisionless conditions of FT-ICR, the intermediate complexes 1 and 2 are chemically activated

k_2: unimolecular isomerization with a *tight* (highy organized) TS (low A factor);
k_{-1} : fragmentation reaction with a *loose* (with many degrees of freedom) TS (high A factor)

energy favors k_2; entropy favors k_{-1}

Negative temperature dependence

competition takes place between one pathway that is energetically favored and another that is entropically favored.

At low E_0 a fast reaction will occur

S. Gronert, Chem. Rev. 2001

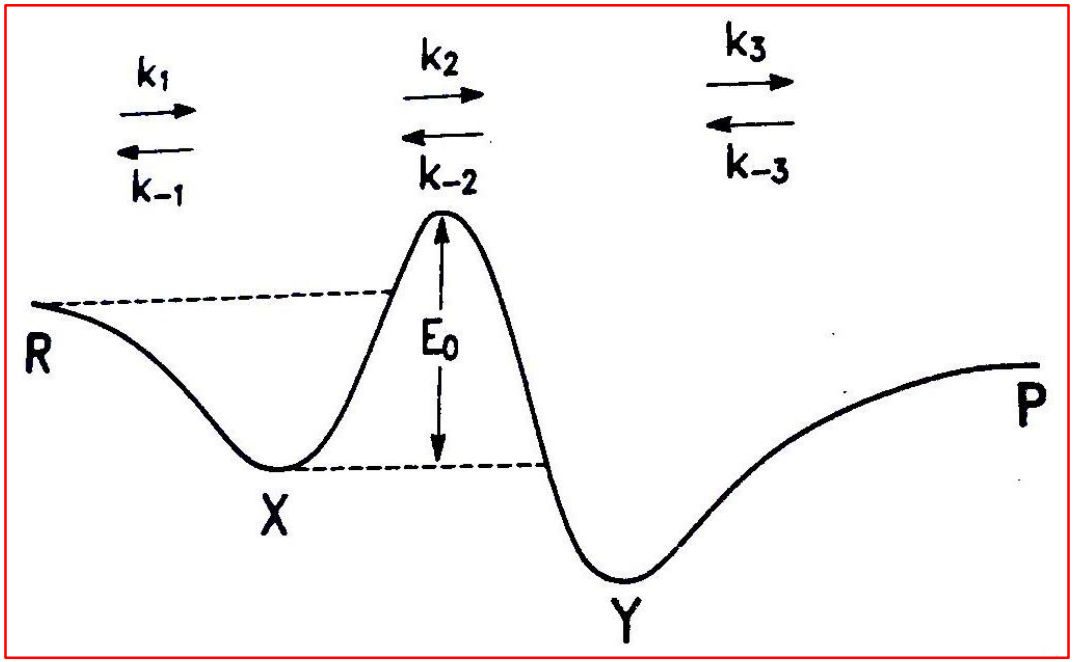

Slow reactions

Double-minimum potential surface with ST lying above the reactants in energy.

For **long-lived** initial complexes, the energy can be removed via emission of a photon (**radiative stabilization**)

Types of Ion-Molecule Reactions

- Electron-Transfer
- Proton transfer
- H-atom/ O-atom transfer
- R^+ transfer
- H/D exchange
- Nucleophilic displacement
- Radiative association

Table 1 Types of ion–molecule reaction

Reaction type	
Electron (charge) transfer	$A^{\pm} + B \rightarrow B^{\pm} + A$
Proton transfer	$AH^+ + B \rightarrow BH^+ + A$
	$A^- + BH \rightarrow AH^{\pm} + B^-$
H-atom transfer	$A^{\pm} + BH \rightarrow AH^{\pm} + B$
R^+ transfer	$AR^+ + B \rightarrow BR^+ + A$
Nucleophilic displacement	$A^- + RX \rightarrow AR + X^-$
Bond redisposition	$AB^{\pm} + C \rightarrow AC^{\pm} + B$
Radiative association	$A^{\pm} + B \rightarrow AB^+ + h\nu$
Collisional association	$A^{\pm} + B + M \rightarrow AB^{\pm} + M$
Switching	$A^{\pm} \cdot B + C \rightarrow A^{\pm} \cdot C + B$
Associative detachment	$A^- + B \rightarrow AB + e$

Proton-Transfer Reactions

$AH^+ + B \rightleftharpoons BH^+ + A$ **kinetics**

$A^- + BH \rightleftharpoons AH + B^-$ **equilibrium**

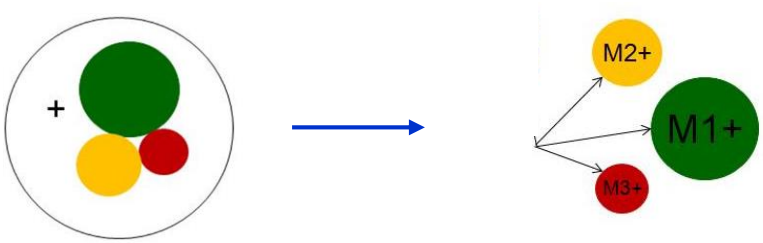

large exothermicity

$BH^+ \longrightarrow M_1^+ + M_2^+ + M_3^+ + \text{neutrals}$

Proton-Transfer Reactions

$$AH^+ + B \rightleftharpoons BH^+ + A$$

base A of unknown GB (PA)

base B of known GB (PA)

by using several reference bases B, the GB (PA) of A can be determined

Bracketing method: kinetics

$$AH^+ + B \longrightarrow BH^+ + A$$

- measurement of k_{exp}
- presence of gaseous B

Equilibrium method: equilibrium

$$AH^+ + B \rightleftharpoons BH^+ + A$$

- measurement of K_{eq}
- presence of gaseous A and B

$$K_{eq} = \frac{[BH]^+ [A]}{[AH]^+ [B]} \qquad \ln K_{eq} = \frac{-\Delta G^\circ}{RT}$$

Thermokinetic method

ELSEVIER

International Journal of Mass Spectrometry and Ion Processes 153 (1996) 37–48

International Journal of Mass Spectrometry and Ion Processes

A relationship between the kinetics and thermochemistry of proton transfer reactions in the gas phase

G. Bouchoux*, J.Y. Salpin, D. Leblanc

Département de Chimie, Laboratorie des Mécanismes Réctionnels, URA CNRS 1307, Ecole Polytechnique, 91128 Palaiseau, Cedex, France

deduce thermochemical information from kinetic data

$$[MH]^+ + B \underset{k_{-1}}{\overset{k_{coll}}{\rightleftharpoons}} [MHB]^+ \xrightarrow{k_1} M + [BH]^+$$

$$k_{exp} = \frac{k_{coll}\ k_1}{k_{-1} + k_1}$$

$$\Phi = \frac{k_{exp}}{k_{coll}} = \frac{1}{1 + (k_{-1} / k_1)}$$

the efficiency is high for highly exoergic reactions and decreases as the transfer approaches thermoneutrality

$$k_i(T) = \frac{k_B T}{h} \exp(-\Delta G_i^{\circ\ddagger}/RT)$$

free energy change for the formation of the activated complex

$$\frac{k_{-1}}{k_1} = \exp(\Delta G_1^{\circ\ddagger}/RT) \qquad \Delta G_1^{\circ\ddagger} = -(\Delta G_{-1}^{\circ\ddagger} - \Delta G_1^{\circ\ddagger})$$

G. Bouchoux, Int. J. Mass Spectrom. Ion Processes 1996

$$\Phi = \frac{k_{exp}}{k_{coll}} = \frac{1}{1 + \exp(\Delta G_l^{0*}/RT)}$$

$$\Delta G_l^{0*} = \Delta G_l^{0} + \Delta G_a^{0}$$

Intrinsic barrier separating reactants and products

free energy for the formation of the activated complex

free energy for a given reaction: **GB(M)-GB(B)**

$$\Phi = \frac{1}{1 + \exp[(\Delta G_l^{0} + \Delta G_a^{0})/RT]}$$

provides a direct link between the kinetic and thermodynamic properties of a proton transfer reaction

a high efficiency is observed for exoergic reactions ($\Delta G_l^0 \leq -20$ kJ mol^{-1})

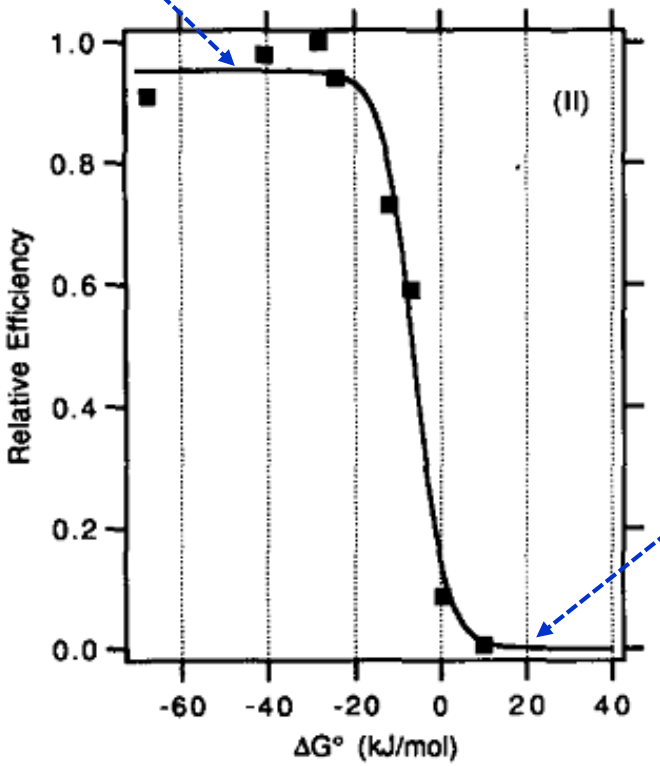

an efficiency close to zero is associated with endoergic processes ($\Delta G_l^0 \geq 10$ kJ mol^{-1})

correlation of Eff with ΔG° allows to determine the unknown GB(M) from a series of experiments involving bases B of known GB

G. Bouchoux, Int. J. Mass Spectrom. Ion Processes 1996

$$H_3SO_3^+ + B_i \rightarrow B_iH^+ + H_2SO_3$$

$$\Delta G^\circ_1 = GB(H_2SO_3) - GB(B_i)$$

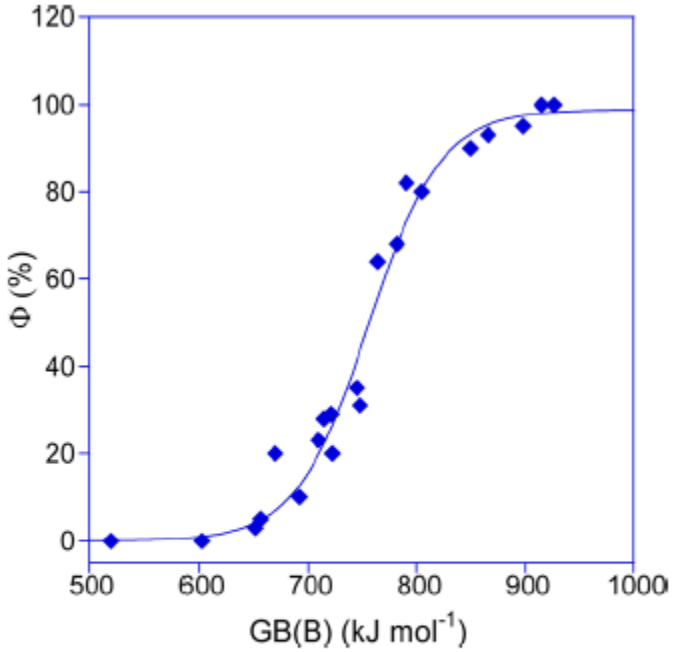

Figure 1. Reaction efficiency (Φ) for the $H_3SO_3^+ + B_i \rightarrow B_iH^+ + H_2SO_3$ proton-transfer reaction plotted versus the GB of the reference bases B_i. The solid curve fits the experimental data based on the parametric function $\Phi = a/\{1 + \exp[(c - GB_{298}(B_i))b]\}$.

H_2SO_3 highly elusive molecule

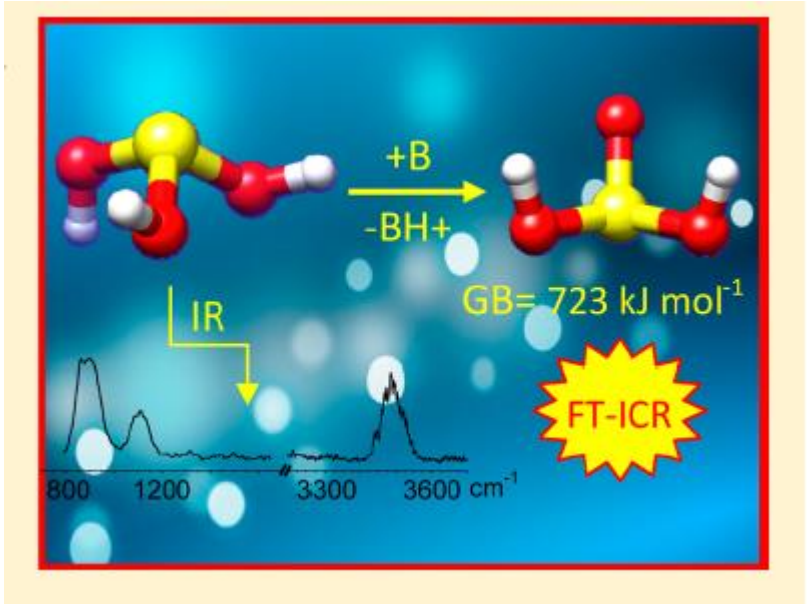

M. E. Crestoni, S. Fornarini et al., J. Phys. Chem. Letters 2015

Chiral recognition in deprotonation reactions

J. Am. Chem. Soc. **1996,** *118,* 8751−8752

Chiral Recognition Is Observed in the Deprotonation Reaction of Cytochrome *c* by (2*R*)- and (2*S*)-2-Butylamine

Elvira Camara, M. Kirk Green, Sharron G. Penn, and Carlito B. Lebrilla*

Department of Chemistry, University of California Davis, California 95616

cyt c + (2R)/(2S)-2-butylamine

(9+, 8+, 7+)

- (2R)- 10 times greater than (2S)-

- one reacting species for 9^+ and two for 8^+ and 7^+ : different conformers

chiral probes of gas-phase structures provide :

- indirect information on protein structures (intermediates of defined structures) and
- thermochemical data about individual sites in large (bio)molecules

Chiral differentiation in host-guest complexes

J. Am. Chem. Soc. **1998,** *120,* 7387−7388

Gas-Phase Chiral Differentiation of Amino Acid Guests in Cyclodextrin Hosts

Javier Ramirez, Fei He, and Carlito B. Lebrilla*

chiral differentiation of AAs is of immediate analytical importance

Scheme 1

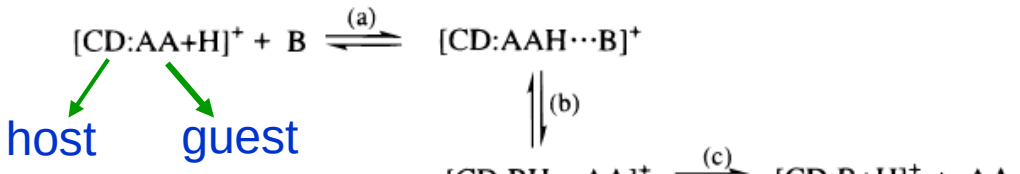

- complexes of protonated β-cyclodextrin-amino acid (Ala; Val; Phe) react with n-propylamine by **exchanging the** AA **guest of cyclodextrin host** for alkylamine;
- the exchange rates are found to differ according to the chirality of the AA
- Valine is the most reactive and shows the greatest selectivity: k_L/k_D= 1.6 (Alanine); k_L/k_D= 3.1 (Valine); k_L/k_D= 0.8 (Phenylalanine).
- **the differences may be related to the way the AA is included into the host cavity.**

C. B. Lebrilla et al., J. Am. Chem. Soc. 1998;
M. Speranza et al. Chiral. 2009

Hydrogen/Deuterium exchange reactions

for counting the active Hs and probe the structure of biomolecules

the ions can be trapped for extended periods of time in the presence of a background pressure of the exchange reagent

to observe H/D exchange, the energy released by complex formation must be sufficient to overcome the barrier to internal PT

$$\text{(Reaction 1)} \quad D_0 + CH_3OD \underset{k_{-1}}{\overset{k_1}{\rightleftharpoons}} D_1 + CH_3OH$$

$$\text{(Reaction 2)} \quad D_1 + CH_3OD \underset{k_{-2}}{\overset{k_2}{\rightleftharpoons}} D_2 + CH_3OH$$

$$\text{(Reaction 3)} \quad D_2 + CH_3OD \underset{k_{-3}}{\overset{k_3}{\rightleftharpoons}} D_3 + CH_3OH$$

$$\text{(Reaction 4)} \quad D_3 + CH_3OD \underset{k_{-4}}{\overset{k_4}{\rightleftharpoons}} D_4 + CH_3OH$$

one approach to analyze the kinetics is the «independent site treatment», where the rate constants are determined iteratively

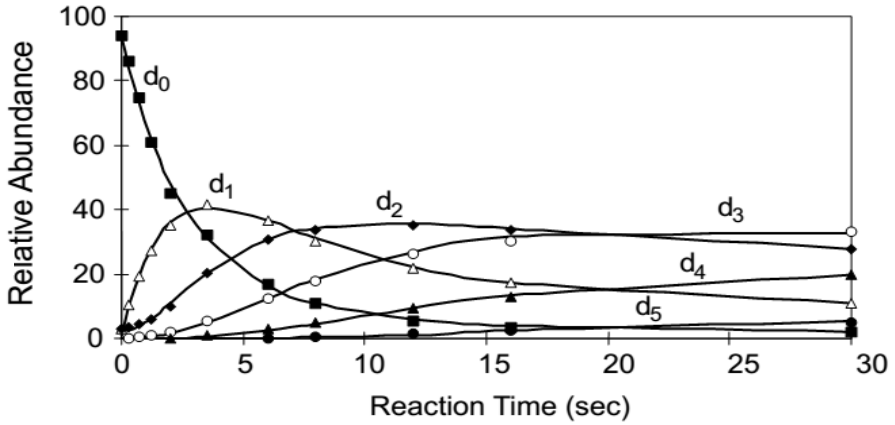

Figure 7. Time plot of the deuterium exchange products of ATP^- reacting with CD_3OD (4.2×10^{-8} mbar)

Table 1. Relative apparent rate constants[a] for the protonated and sodiated adenine nucleotides with reagent gases

Parent ion	m/z	Rea
$AMPH^+$	348	CD
$ADPH^+$	428	
$ATPH^+$	508	

One advantage:

- H/D exchange probes several sites in a molecule (proton transfer involves a single site)

C. B. Lebrilla et al., *MSR* 1997

M. E. Crestoni, S. Fornarini, *J. Mass Spectrom.* 2003

Gas-phase H/D exchange of proteins

The structural and dynamic properties of protein ions (multiply charged ions of cyt c) have been probed by H/D exchange with D_2O in a FT-ICR

At least three distinct gaseous conformers were distinguished by the number of exchangeable Hs : 52, 113 and 74 reactive Hs atoms, possibly corresponding to solution conformers III (native), II (denatured, unfolded), and I (denatured, folded).

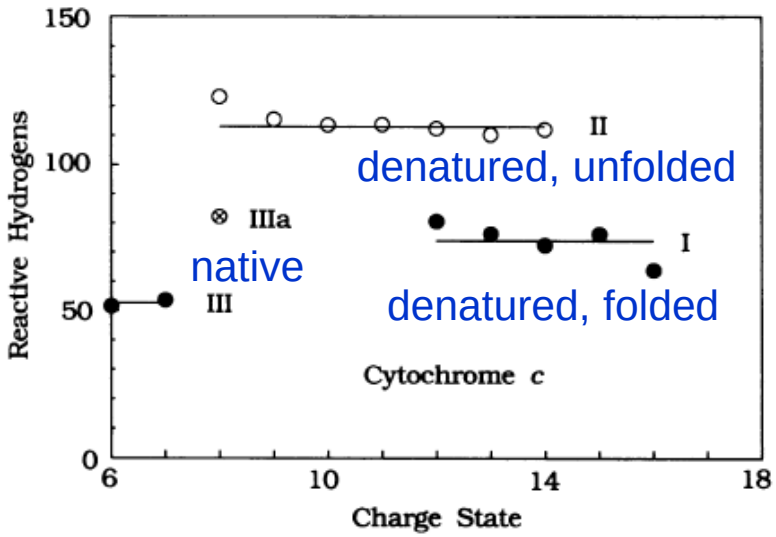

FIG. 3. Number of reactive H atoms observed for possible conformers of cytochrome *c*.

These forms do not interconvert in hours and are stabilized by intramolecular non-covalent interactions of similar nature both in solution and in vacuo.

F. W. McLafferty et al., *PNAS USA* 1993

The use of chemical ionization is the most common **application of IMR in analytical MS for the identification of functional groups in organic compounds**.

Besides proton transfer reagents, alternative reagents has been developed allowing selective reactions, like methylation, vinylation, metal attachment and so on, to be carried out.
Some examples are following...

Identification of functional groups in organic compounds

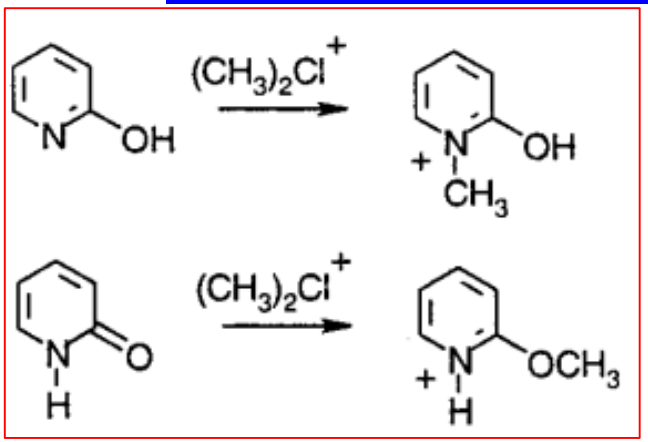

identification via CID of independently synthetized products

O'Hair, Eur. J. Mass Spetrom. 1995

ELSEVIER
International Journal of Mass Spectrometry and Ion Processes 141 (1995) 229–240
International Journal of Mass Spectrometry and Ion Processes

Differentiation of stereoisomeric diols by using $CH_3OB^+OCH_3$ in a small Fourier transform ion cyclotron resonance mass spectrometer

D.T. Leeck[a], T.D. Ranatunga[a], R.L. Smith[a], T. Partanen[b], P. Vainiotalo[b,*], H.I. Kenttämaa[a,*]

cis-1,2-cyclo pentanediol

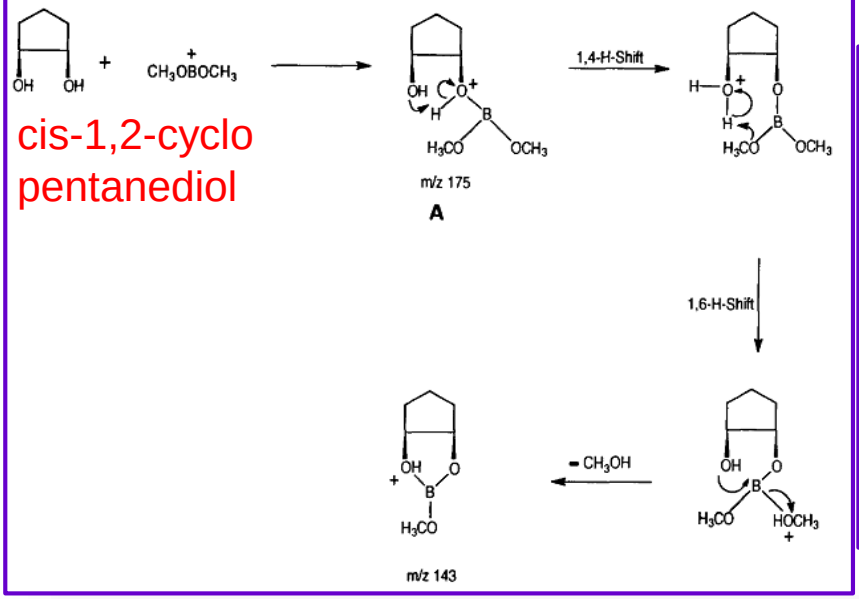

trans

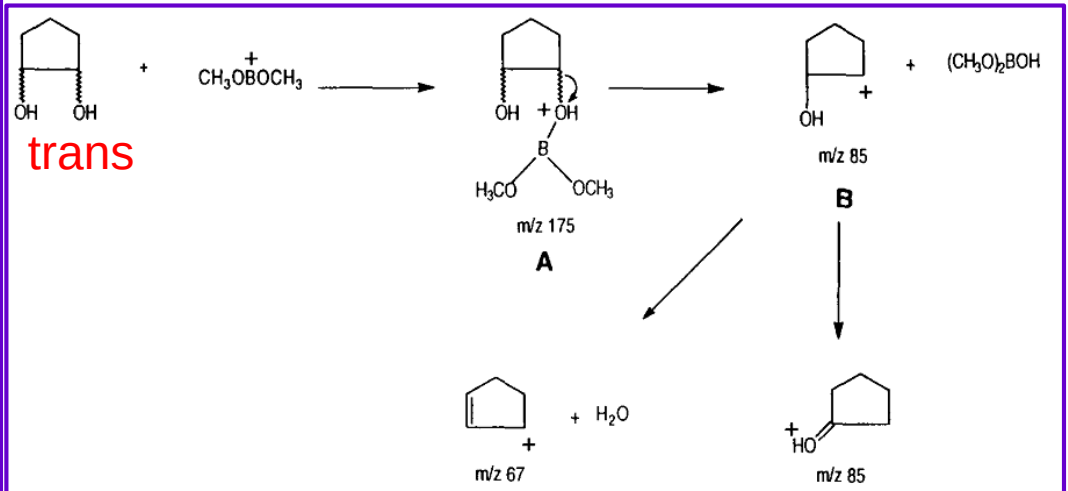

O'Hair, Eur. J. Mass Spetrom. 1995;
H. I. Kenttamaa, *Int. J. Mass Spectrom. Ion Proc.* 1995

Anal. Chem. **2004,** *76,* 964−976

Ion−Molecule Reactions for Mass Spectrometric Identification of Functional Groups in Protonated Oxygen-Containing Monofunctional Compounds

Michael A. Watkins,[†] Jason M. Price,[†,‡] Brian E. Winger,[§] and Hilkka I. Kenttämaa*[,†]

1) ethyl vinyl ether
2) diethylmethoxyborane

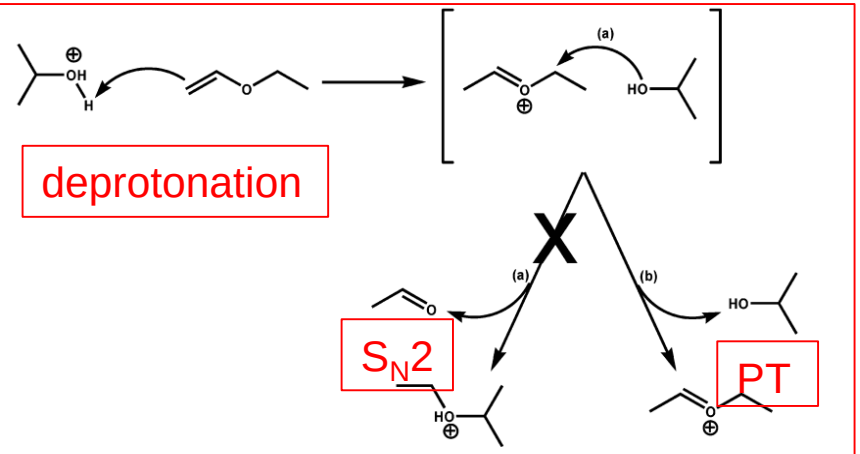

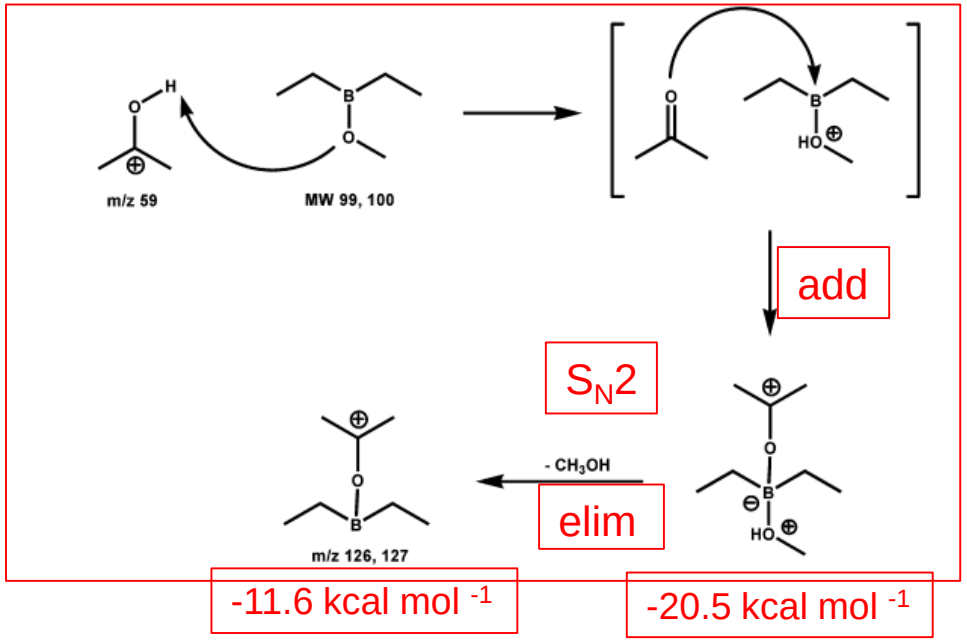

diethylmethoxyborane reacts with protonated monofunctional oxygen-containing analytes (**alcohols, ketones, aldehydes, esters, ethers, carboxylic acids, amides**) by deprotonation followed by substitution of methanol: provides structure elucidation for unknown mixture components

Identification of functional groups in organic compounds

J. Am. Soc. Mass Spectrom. (2012) 23:12-22
DOI: 10.1007/s13361-011-0249-y

RESEARCH ARTICLE

Identification of Epoxide Functionalities in Protonated Monofunctional Analytes by Using Ion/Molecule Reactions and Collision-Activated Dissociation in Different Ion Trap Tandem Mass Spectrometers

Ryan J. Eismin, Mingkun Fu, Sonoeun Yem, Fanny Widjaja, Hilkka I. Kenttämaa
Department of Chemistry, Purdue University, 560 Oval Drive, West Lafayette, IN 47907, USA

TMB is able to depronate O functionalities but not N groups

Vinyl and phenyl epoxides can be differentiated from other O-containing analytes, based on the **loss of a second methanol molecule** upon CID of the addition/methanol elimination product.

IMR involves **proton transfer** from the protonated analyte to TMB, followed by **addition** of the analyte to TMB and **elimination** of methanol

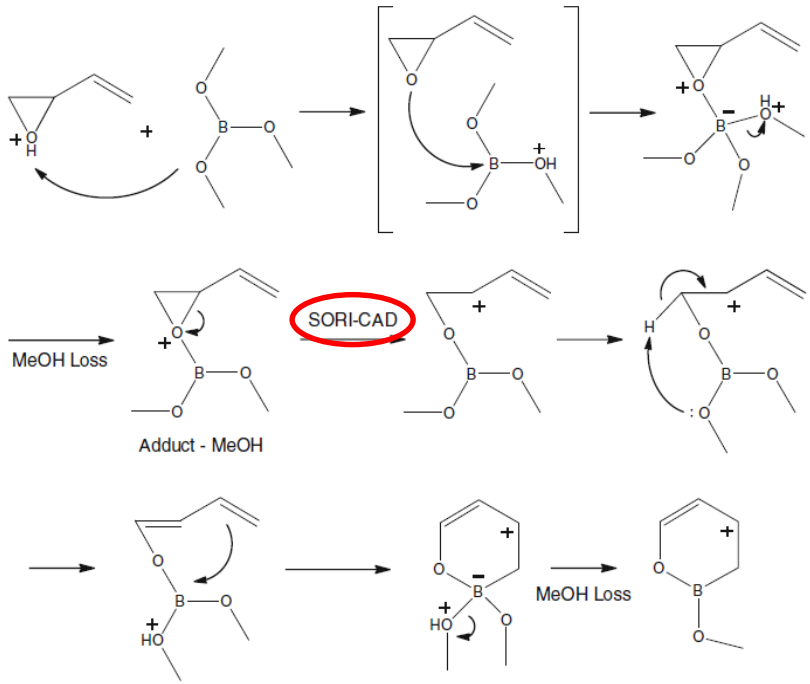

Mechanism for elimination of two methanol molecules upon reaction of protonated butadiene monoxide with TMB

Anal. Chem. **2005,** *77,* 5311−5316

Compound Screening for the Presence of the Primary *N*-Oxide Functionality via Ion−Molecule Reactions in a Mass Spectrometer

Michael A. Watkins,† Danielle V. WeWora,† Sen Li,† Brian E. Winger,‡ and Hilkka I. Kenttämaa*,†

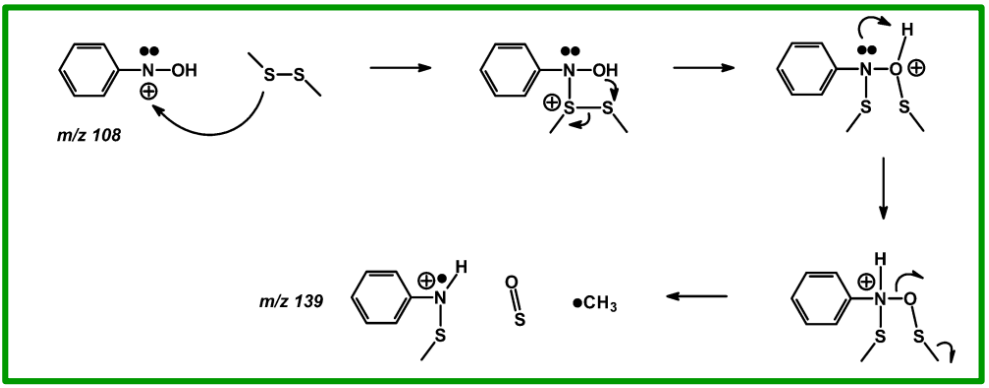

protonated primary N-oxides selectively react with $(CH_3S)_2$ forming a product with 31 Da higher mass.

JOC *Article*

J. Org. Chem. **2008**, *73*, 4888–4894

Identification of the Aromatic Tertiary *N*-Oxide Functionality in Protonated Analytes via Ion/Molecule Reactions in Mass Spectrometers

Penggao Duan,† Todd A. Gillespie,‡ Brian E. Winger, and Hilkka I. Kenttämaa*,†

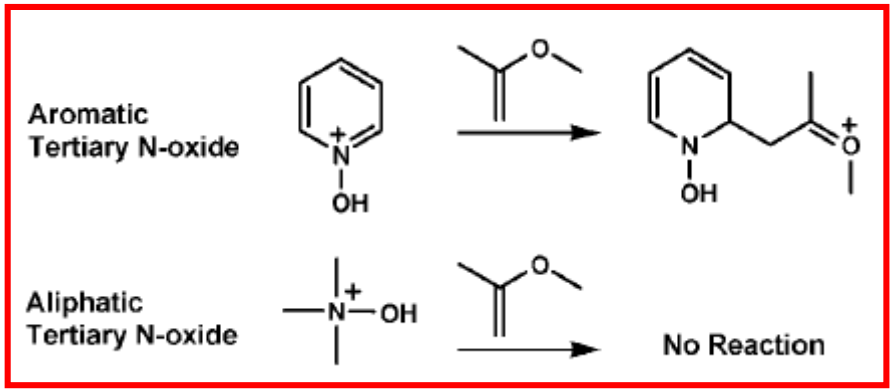

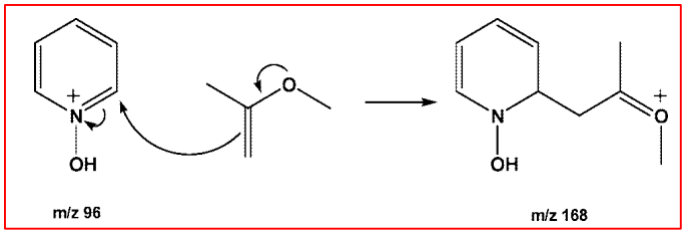

protonated aromatic tertiary N-oxides selectively add 2-methoxy-propene

JOC *Article*

J. Org. Chem. **2009**, *74*, 1114–1123

Identification of Aliphatic and Aromatic Tertiary N-Oxide Functionalities in Protonated Analytes via Ion/Molecule and Dissociation Reactions in an FT-ICR Mass Spectrometer

Penggao Duan,† Mingkun Fu,† Todd A. Gillespie,‡ Brian E. Winger,‡ and Hilkka I. Kenttämaa*,†

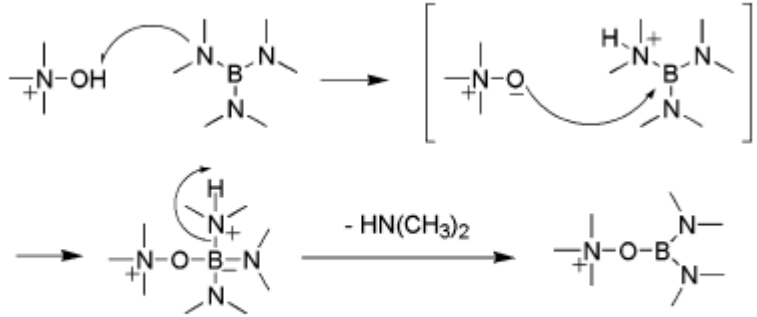

Scheme 1. Mechanism proposed for the reaction between protonated N-oxide containing analyte and neutral TDMAB.

aliphatic and aromatic tertiary N-oxides react with tri(dimethylamino)borane yielding add-elim products identified via SORI-CID

Journal of Pharmaceutical and Biomedical Analysis 51 (2010) 805–811

Contents lists available at ScienceDirect

Journal of Pharmaceutical and Biomedical Analysis

journal homepage: www.elsevier.com/locate/jpba

Liquid chromatography/tandem mass spectrometry utilizing ion-molecule reactions and collision-activated dissociation for the identification of N-oxide drug metabolites

Steven C. Habicht, Penggao Duan[1], Nelson R. Vinueza, Mingkun Fu, Hilkka I. Kenttämaa*

Department of Chemistry, Purdue University, West Lafayette, IN 47907, USA

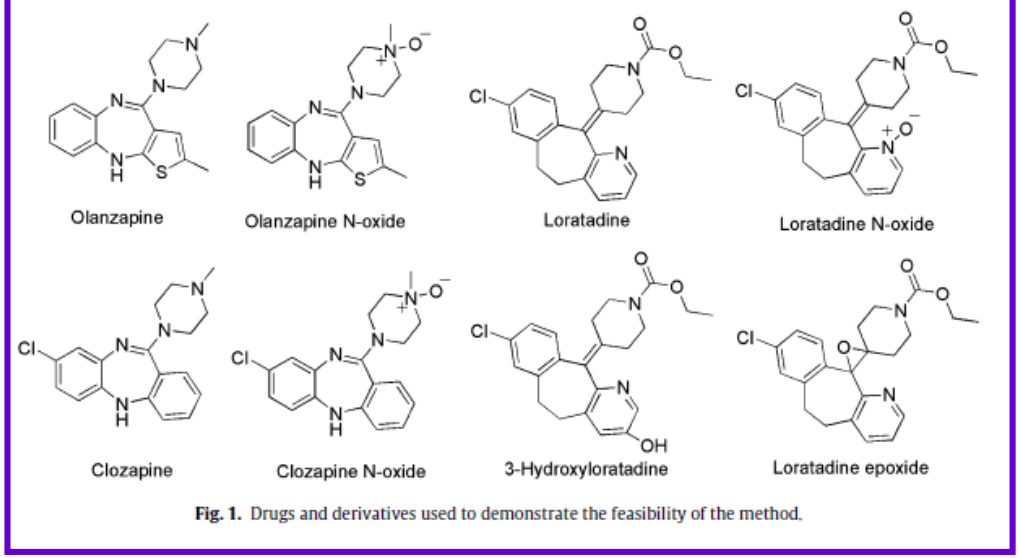

Fig. 1. Drugs and derivatives used to demonstrate the feasibility of the method.

application in the pharmaceutical setting

Identification of functional groups in biomolecules

S. A. McLuckey, *Anal. Chem.* 1997

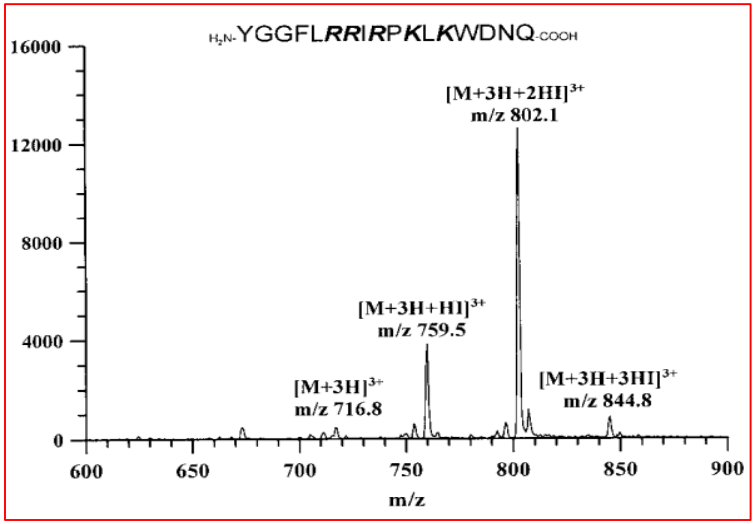

the adducts possess as many HI units as the total number of basic AAs (arginine, lysine) and the N-terminus

Research Article

Rapid Communications in Mass Spectrometry

Received: 25 January 2014 Revised: 27 February 2014 Accepted: 27 February 2014 Published online in Wiley Online Library

Rapid Commun. Mass Spectrom. **2014**, *28*, 1107–1116
(wileyonlinelibrary.com) DOI: 10.1002/rcm.6884

Probing the exposure of the phosphate group in modified amino acids and peptides by ion-molecule reactions with triethoxyborane in Fourier transform ion cyclotron resonance mass spectrometry

Francesco Lanucara[1,2*], Simonetta Fornarini[3], Claire E. Eyers[2] and Maria Elisa Crestoni[3]

$[\text{Peptide-O-P(O)(OH)}_2\text{+nH}]^{n+} + \text{B(OR)}_3 \rightarrow [\text{Peptide-O-PO(OH)OB(OR)}_2\text{+nH}]^{n+} + \text{ROH}$

Scheme 1. Addition-elimination reaction of phosphorylated amino acids and peptides with alkoxyboranes $B(OR)_3$.

set of phosphorylated peptides comprising phosphorylated serine and threonine, bearing a C-terminus lysine or arginine residue and holding naturally occurring sequences

Potential to measure the effect of local environment, the exposure and accessibility of a phosphate moiety on the surface of a biomolecule and to distinguish positional phosphorylated peptide isomers

The efficiency of such reactions allows to explore the accessibility of phosphate groups in biomolecules

S. A. McLuckey et al., *Anal. Chem.* 1997;
Lanucara et al., *Rapid Commun. Mass Spectrom.* 2014

Identification of functional groups in biomolecules

J Biol Inorg Chem (2007) 12:22–35
DOI 10.1007/s00775-006-0159-9

ORIGINAL PAPER

Heme-peptide/protein ions and phosphorous ligands: search for site-specific addition reactions

Maria Elisa Crestoni · Simonetta Fornarini

Effect of axial ligand: free and ligated heme-type ions

- **Fe(III)-heme$^+$**
- **MP11**
- **cyt c**
- **myoglobin**

+ $OP(OMe)_3$ (GB: 206 kcal/mol)
+ $P(OMe)_3$ (GB: 215.3 kcal/mol)

insight in the coordination environment of the prosthetic group in systems of increasing complexity

the addition of phosphite is always limited to just one molecule, irrespective of charge state, in contrast with a charge-dependent number of added phosphate ligands

- **$OP(OMe)_3$ is engaged in H bonding to protonated sites**
- **$P(OMe)_3$ is sampling the protein prosthetic group**

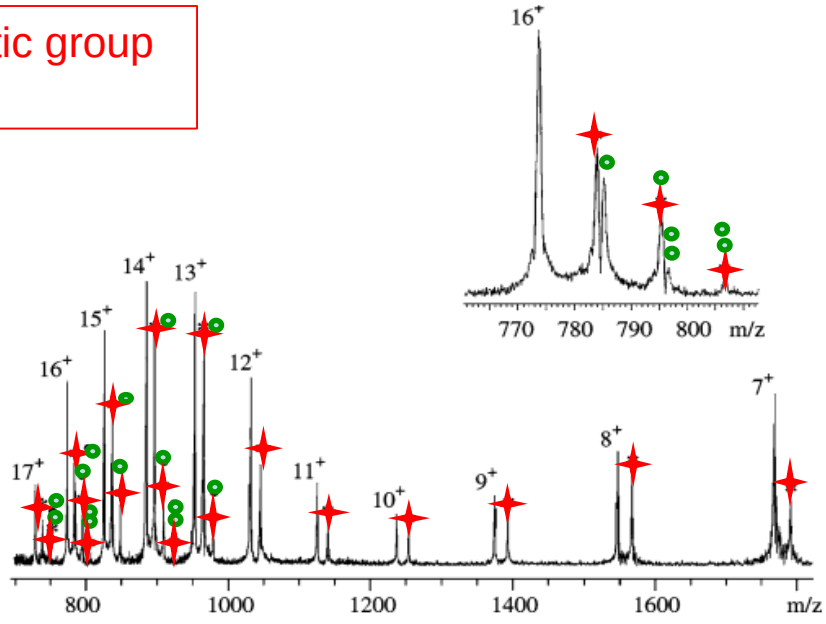

Fig. 9 FT-ICR mass spectrum of cyt *c* allowed to react with a 70:30 mixture of triethylphosphite, $P(OEt)_3$, and triethylphosphate, $OP(OEt)_3$, at 2.4×10^{-8} mbar for 3 s. *Numbers* denote the charge states of cyt *c* ions. Each charge state forms adducts with a single $P(OEt)_3$ molecule (represented by a *star*). The high charge states add up to four $OP(OEt)_3$ molecules; each $OP(OMe)_3$ molecule is represented by a *circle*

The naked core of Cpd I

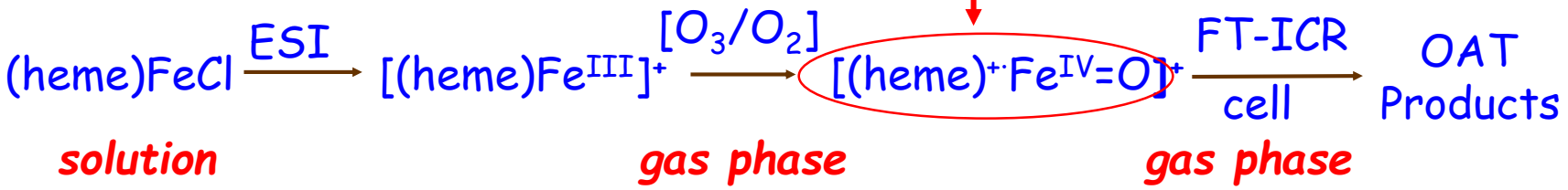

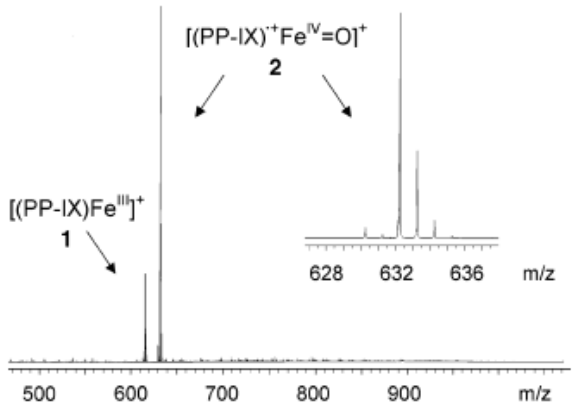

Figure 1. ESI FT-ICR mass spectrum from a methanol solution o (PP-IX)FeCl (10 μM), admitting O_3/O_2 in the capillary/skimmer interface of the ESI source. The inset is an enlargement of the spectrum displaying signals characteristic of $(PP\text{-}IX)^{+\bullet}Fe^{IV}$=O ions (**2**).

Ion-molecule reactions of $[(heme)^{+\cdot}Fe^{IV}=O]^+$

Table 1. Gas-Phase Reactivity of Selected Substrates (L) with $(PP\text{-}IX)^{+\bullet}Fe^{IV}(O)^+$ (**2**) Formed by the Reaction of $Fe(PP\text{-}IX)^+$ (**1**) with O_3

L	k_{exp}[a]	Φ[b]	product ions **1**/(PP-IX)Fe(O)(L)$^+$
NO	3.0	4.2	100/0
NO_2	1.9	2.9	100/0
propyne	0.036	0.027	100/0
Me_2S	1.7	1.3	80/20
Me_2S_2	2.8	2.4	90/10
pyridine	2.4	1.7	100/0
$P(OMe)_3$	8.6	7.3	95/5

Oxophilic Character

C

N

S

P

M. E. Crestoni, S. Fornarini, *Inorg. Chem.* **2007**

Association Reactions

- solvation of an ion by weak electrostatic or hydrogen bonding;
- ion ligation involving bonds of intermediate strength;
- strong chemical bond formation

$$A^{\pm} + B \rightleftharpoons (AB)^{\pm *}$$

$$(AB)^{\pm *} \longrightarrow AB^{\pm} + h\nu \dashrightarrow \text{FT-ICR}$$

$$(AB)^{\pm *} + M \longrightarrow AB^{\pm} + M \dashrightarrow \text{Ion-trap}$$

at the low operating pressures of the FT-ICR cell: thermal equilibration of the adduct ion via IR radiative emission

The rate of radiative emission is expected to increase with increasing size of the ion

F.W. Mc Lafferty et al., *J. Am. Chem. Soc. 2001*

(J Am Soc Mass Spectrom 2005, 16, 589–598)

Binding of Gaseous Fe(III)-Heme Cation to Model Biological Molecules: Direct Association and Ligand Transfer Reactions

Fausto Angelelli, Barbara Chiavarino, Maria Elisa Crestoni, and Simonetta Fornarini

Department of Studies on Chemistry and Technology of Biologically Active Substances, University of Rome, "La Sapienza," Rome, Italy

Ligand association equilibrium

$$\text{Fe(III)-heme}^+ + \text{L} \underset{k_{-1}}{\overset{k_1}{\rightleftarrows}} \text{Fe(III)-heme(L)}^+$$

L= NO, amines, carbonyl compounds, ethers, nitriles, sulfides, phosphoryl compounds

$$HCB(L) = -\Delta G^\circ = -RT\ln K_{eq}$$

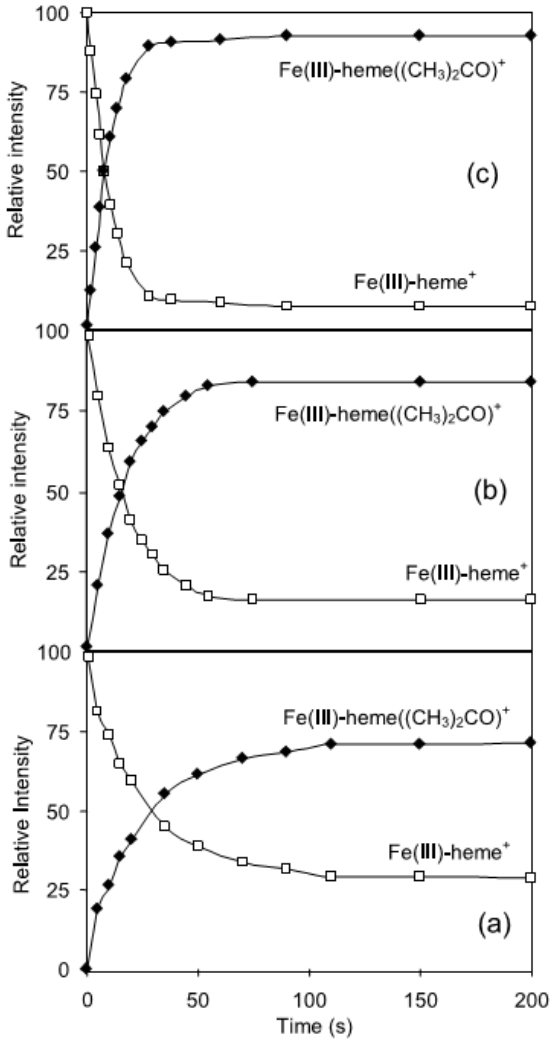

Figure 5. Time dependence of ion abundances for the Fe(III)-heme$^+$ ion reaction with acetone at 5.2×10^{-8} mbar (**a**), 8.7×10^{-8} mbar (**b**), 2.1×10^{-7} mbar (**c**).

Ligand transfer equilibria

$$Fe(III)\text{-}heme(L_1)^+ + L_2 \rightleftarrows Fe(III)\text{-}heme(L_2)^+ + L_1$$

$$HCB(L_1) - HCB(L_2) = -\Delta G^\circ = -RT\ln K_{eq}$$

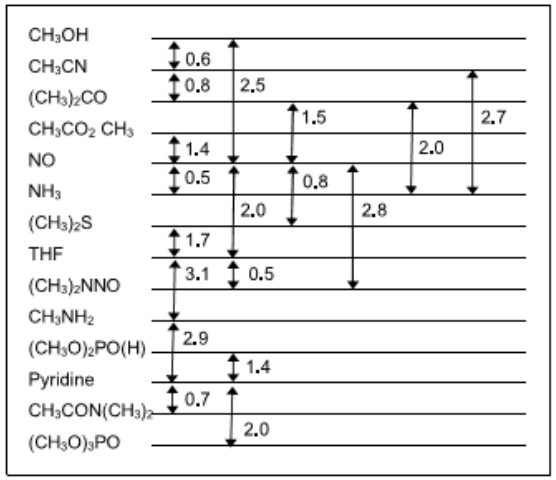

Figure 7. ΔG_5° (kcal mol^{-1}, 300 K) ladder for the Fe(III)-heme$^+$ transfer reactions between selected pairs of ligands. The values in the ladder correspond to HCB differences for each couple of ligands.

Table 6. Free energy changes for gas-phase ligand binding toward H^+ and Fe(III)-heme$^+$

L	GB[a]	HCB[b]
CH_3OH	173.2	13.1
CH_3CN	179.0	13.7
$(CH_3)_2CO$	186.9	14.6
CH_3CO_2 CH_3	189.0	14.8
NO	120.8	16.1
NH_3	195.7	16.6
$(CH_3)_2S$	191.5	
Tetrahydrofuran	189.9	
$(CH_3)_2N$-NO	203.0[c]	
CH_3NH_2	206.6	
$(CH_3O)_2PO(H)$	206.1	
Pyridine	214.7	
$CH_3CON(CH_3)_2$	209.6	
$(CH_3O)_3PO$	205.7	

A linear correlation between HCBs and ΔGBs of the ligands suggests that similar effects play a role when a lone pair donor binds to a proton or to Fe(III)heme$^+$

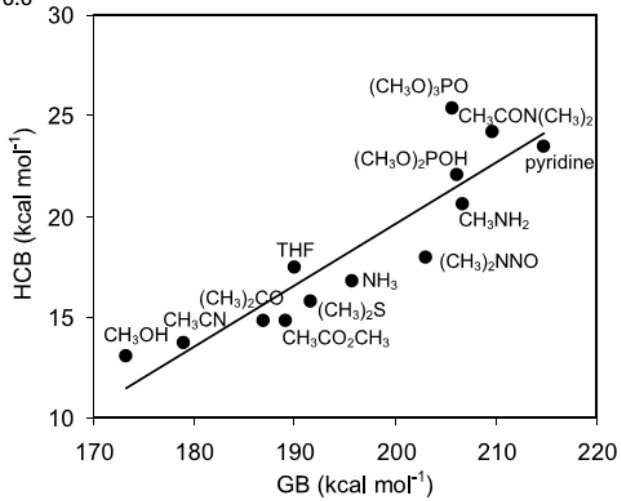

Figure 9. General correlation between Fe(III)-heme$^+$ cation basicities (HCB, equal to $-\Delta G_1^\circ$ for the ligand association reaction) and gas phase basicity toward the proton (GB) values.

NO binding to Fe(II) and Fe(III)-hemes

Inorg. Chem. **2008**, *47*, 7792−7801

Inorganic Chemistry
Article

Unravelling the Intrinsic Features of NO Binding to Iron(II)- and Iron(III)-Hemes

Barbara Chiavarino,[†] Maria Elisa Crestoni,[†] Simonetta Fornarini,*[,†] and Carme Rovira*[,‡]

Table 1. Rate and equilibrium constants for NO binding to iron(II)/iron(III) porphyrin complexes and heme proteins[9]

Iron(II)/(III) porphyrin[(a)]	k_f / M^{-1} s^{-1}	k_r / s^{-1}	K / M^{-1}
Mb(II)	1.7×10^7	1.2×10^{-4}	1.4×10^{11}
Mb(III)	1.9×10^5	13.6	1.4×10^4
Hb(II)	2.5×10^7	4.6×10^{-5}	5.3×10^{11}
Hb(III)	4×10^3	1	4×10^3
Fe^{II}(TPPS)	1.8×10^9	≈ 0	$> 10^9$
Fe^{III}(TPPS)	7.2×10^5	6.8×10^2	1.1×10^3
Fe^{II}(TMPS)	1×10^9	–	–
Fe^{III}(TMPS)	3×10^6	7.3×10^2	4.1×10^3

[(a)] Mb: myoglobin; Hb: hemoglobin; TPPS: meso-tetra(4-sulfonatophenyl)porphyrinato dianion; TMPS: meso-tetra(sulfonatomesityl)porphyrinato dianion.

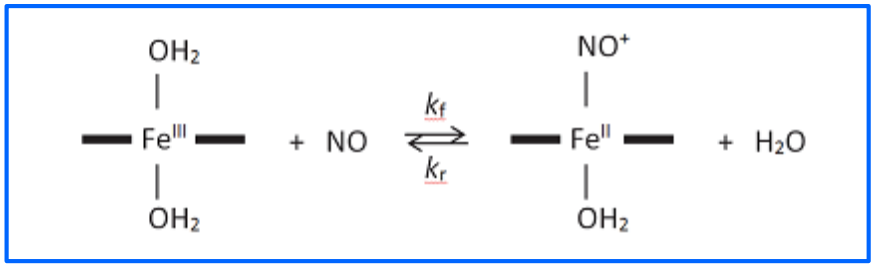

NO addition is governed by:
- Fe coordination number
- Fe oxidation state

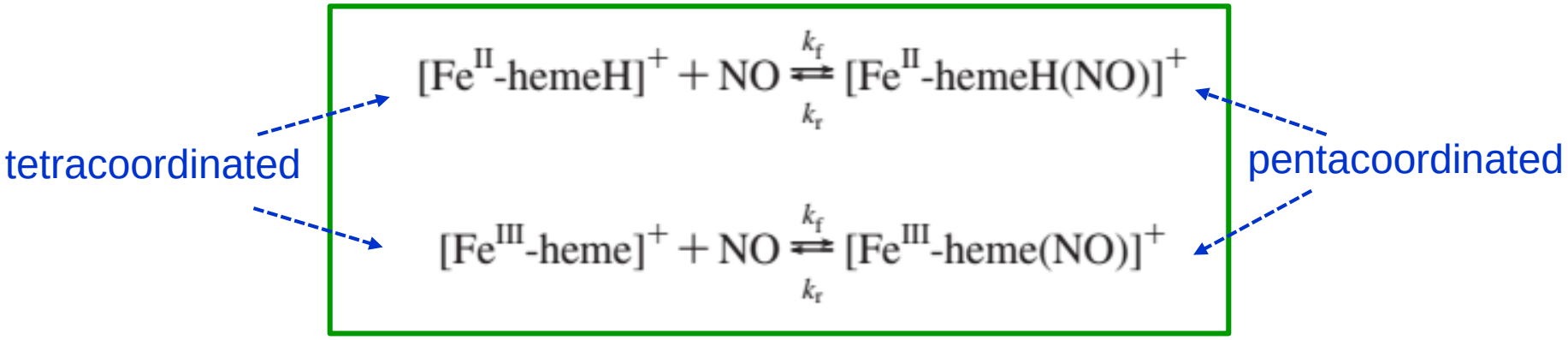

Table 4. Kinetics and Equilibrium Data for NO Binding to $[Fe^{II}\text{-hemeH}]^+$ and $[Fe^{III}\text{-heme}]^+$ Ions in the Gas Phase

reagent ion	K_1 ($\times 10^{-11}$)[a]	k_f ($\times 10^{11}$)[b]	k_r ($\times 10^{3}$)[c]
$[Fe^{II}\text{-hemeH}]^+$	5.7	3.3	0.8
$[Fe^{III}\text{-heme}]^+$	5.3	2.2	0.9

[a] Equilibrium constant for the association of NO to the heme ions at 300 K, obtained from the $H^{II}CB/H^{III}CB$ values reported in Table 3 (K_1 = exp(HCB/RT)). Standard state 1 atm. [b] Forward rate constant for the association of NO to the heme ions, in units of cm^3 $molecule^{-1}$ s^{-1}, at 300 K. refs 8b and 10. [c] Reverse rate constant for the association of NO to the heme ions, in s^{-1}, at 300 K. This work.

$HCB^{II}_{(NO)} = HCB^{III}_{(NO)} = 67$ kJ mol $^{-1}$ at 300 K

both oxidation states show similar kinetic and thermodynamic behaviour

S. Fornarini et al. Inorg. Chem. 2008

Ion-molecule reactions of radical cations

J|A|C|S
ARTICLES
Published on Web 02/23/2005

Reactions of Charged Phenyl Radicals with Aliphatic Amino Acids in the Gas Phase

Yiqun Huang, Leo Guler, Jenny Heidbrink, and Hilkka Kenttämaa*

Contribution from the Brown Laboratories, Department of Chemistry, Purdue University, 425 Central Drive, West Lafayette, Indiana 47907-2018

distonic ion approach

phenyl radicals with a chemically inert, charged substituent remote from the radical site display the same reactions as the corresponding neutral radicals

the charged group is the essential handle for MS manipulations

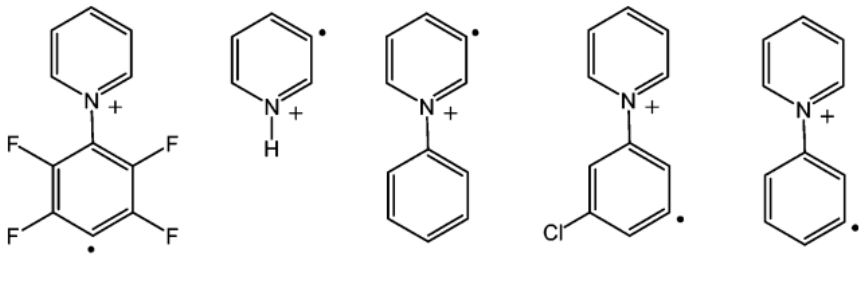

Figure 1. Positively charged phenyl radicals used in this study.

EA ordering of radicals:

A (6.2 eV) > B (6.1 eV) > C (5.8 eV) > D (5.1 eV) > E (4.9 eV)

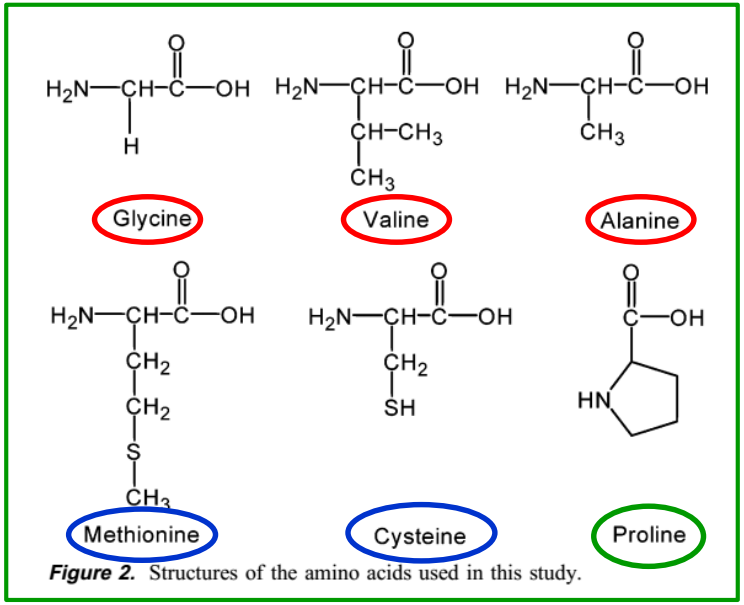

Figure 2. Structures of the amino acids used in this study.

H. I. Kenttamaa, *J. Am. Chem.* 2005

Ion-molecule reactions of radical anions

J. Am. Soc. Mass Spectrom. (2011) 22:1794–1803
DOI: 10.1007/s13361-011-0198-5

RESEARCH ARTICLE

Structure and Reactivity of the *N*-Acetyl-Cysteine Radical Cation and Anion: Does Radical Migration Occur?

Sandra Osburn,[1] Giel Berden,[2] Jos Oomens,[2,3] Richard A. J. O'Hair,[4,5,6] Victor Ryzhov[1]

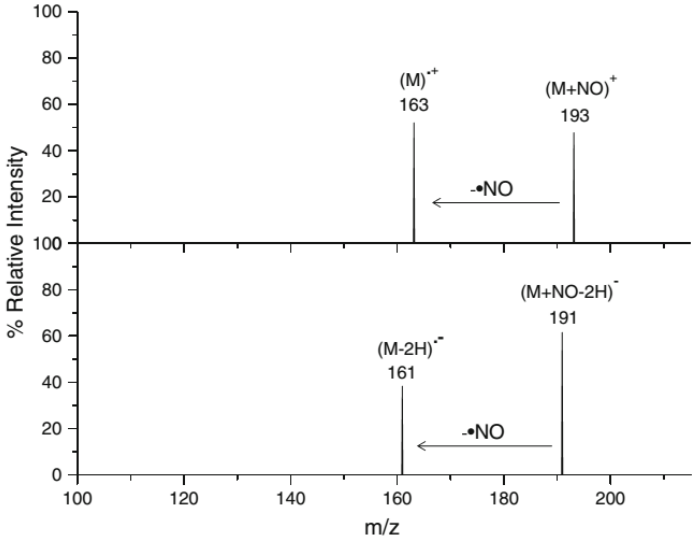

Figure 1. CID of nitrosylated *N*-acetyl-cysteine ion to generate the radical (**a**) cation and (**b**) anion of acetyl cysteine

$M^{\cdot+} + CH_3SCH_3 \longrightarrow (M+CH_3)^+ + \cdot SCH_3$

$(M+allyl)^+ + \cdot CH_2CHCH_2$

$(M+allyl)^+ + \cdot CH_2CHCH_2$

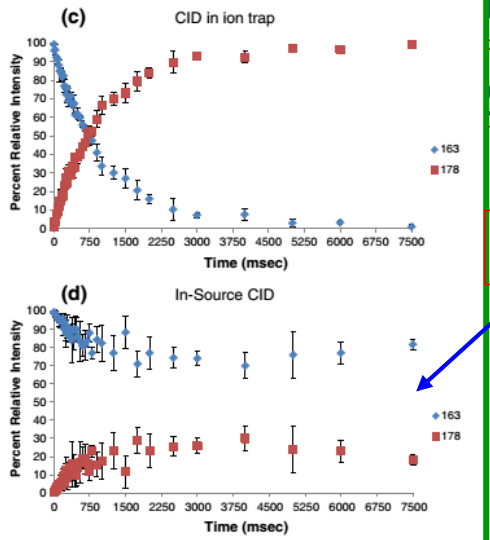

Figure 4. Mass spectrum of the radical cation of *N*-acetyl-cysteine formed via (**a**) CID and (**b**) in-source fragmentation reacting with dimethyl sulfide. Pressure of the neutral is ca. 10^{-7} Torr, reaction time is 800 ms. Kinetic plots of the radical cation formed via (**c**) CID and (**d**) in-source fragmentation reacting with dimethyl sulfide

in-source fragmentation: the radical migrates from S to the α-C

$(M-2H)^{\cdot-} + CH_3SSCH_3 \longrightarrow (M-2H+SCH_3)^- + \cdot SCH_3$

$(M-2H)^{\cdot-} + allylBr \longrightarrow (M-2H+allyl)^- + \cdot CH_2CHCH_2$

$(M-2H)^{\cdot-} + allylI \longrightarrow (M-2H+allyl)^- + (M-2H+I)^- + \cdot CH_2CHCH_2$

- **Who :** EU_FT-ICR_MS
- **What :** **Short Course 3 (SC3)** on **Ion/molecule reactions: fundamental and analytical aspects**
- **When :** june 2019 (M18)

- **Where :** Roma (Italy) at Sapienza University

- **Why:** deepen the study and applications and perfom experiments on IMR

SAPIENZA
UNIVERSITÀ DI ROMA



SC3, June 2019

EU FT-ICR MS






Simonetta Fornarini

Dip. CTF's Colleagues

Thank you for your kind attention

Hope to see all of you in Roma in 2019 !